Coherent control of magnetization via inverse Faraday effect

2006 J. Phys.: Condens. Matter 18 7063

(http://iopscience.iop.org/0953-8984/18/31/002)

INSTITUTE OF PHYSICS PUBLISHING JOURNAL OF PHYSICS: CONDENSED MATTER

J. Phys.: Condens. Matter **18** (2006) 7063–7078 doi:10.1088/0953-8984/18/31/002

Coherent control of magnetization via inverse Faraday effect

C A Perroni and A Liebsch

Institut für Festkörperforschung (IFF), Forschungszentrum Jülich, 52425 Jülich, Germany

Received 29 April 2006, in final form 13 June 2006
Published 21 July 2006
Online at stacks.iop.org/JPhysCM/18/7063

Abstract
Recent experiments have demonstrated the possibility of ultrafast non-thermal control of magnetization in rare-earth orthoferrites and ferrimagnetic garnet films via circularly polarized femtosecond laser pulses. Single and double pump pulses set up ultrafast magnetic fields via the inverse Faraday effect, thereby non-thermally exciting spin dynamics. A theoretical study of coherent control of the magnetization in rare-earth orthoferrites is performed by considering the effect of multiple pulses. The investigation is based on a model for orthoferrites recently proposed for the study of the inverse Faraday effect in the case of a single pump pulse. In the linear regime without damping, interferential effects take place: in-phase pulses induce a coherent enhancement of magnetization. The role of relaxation and nonlinearity is studied in relation to their capability of hampering coherent manipulation of magnetization. After many pulses, the effect of damping induces a stationary behaviour with a periodicity determined by the separation time between successive pulses. Due to nonlinear effects, the magnetization can be characterized by complex beating patterns whose amplitude and periodicity depend on the intensity of exciting pulses.

1. Introduction

In recent years the tremendous increase in speed of magneto-optic devices and in magnetic storage density has triggered many studies aimed at understanding the mechanisms of magnetization dynamics and switching on timescales of a picosecond or less. Ultrafast optical laser pulses are currently used to manipulate the magnetization on the scale of a few hundred femtoseconds. Actually, a significant demagnetization of metallic ferromagnetic compounds can be induced by the absorption of the laser light on this short timescale [1–4]. In metals the light absorption gives rise to a rapid increase of temperature and the electrons are excited to high energy bands. Due to inter-particle interaction, during the relaxation the electrons rapidly lose their coherence and the magnetization can only follow the thermal behaviour. Therefore, during this process, the magnetization cannot be controlled.

Recently, the ultrafast non-thermal control of magnetization has become feasible in insulating canted antiferromagnets by using circularly polarized femtosecond laser pulses [5]. As a result of the inverse Faraday effect, these pulses set up a magnetic field (of the order of 0.5 T) directed along the wavevector of the radiation and proportional to its intensity [6, 7]. The pulses non-thermally excite the nearly transparent system and coherently control the spin dynamics. Stimulated by these results, a theoretical study of magnetization dynamics in rare-earth orthoferrites was performed by solving Landau–Lifshitz–Gilbert equations [8]. This approach provided results compatible with experimental findings.

The inverse Faraday effect also plays a role in the femtosecond photomagnetic switching of spins in ferromagnetic garnet films [9]. The coherent optical control of the magnetization of these compounds has been demonstrated by employing double pump pulses in rapid succession [10]. In this experiment two circularly polarized pump pulses with opposite helicities and almost equal powers were used. Depending on the phase of the magnetization at the time when the second pulse arrives, stopping of the dynamics as well as doubling of the amplitude can be achieved. Another example of optical control could take place in antiferromagnets: a theoretical proposal was made for ultrafast all-optical magnetic switching by using shaped short laser pulses [11]. These effects open exciting possibilities to manipulate directly and coherently spin dynamics by using multiple laser pulses.

In order to obtain a deeper understanding of the coherent control of magnetization dynamics, in this paper simulations are discussed for double and multiple pulses. The studied systems are rare-earth orthoferrites. The magnetization dynamics of these compounds is studied employing an approach that has been recently proposed for the analysis of inverse Faraday effect due to a single pump pulse [8]. The dynamical behaviour is determined by solving two coupled sublattice nonlinear Landau–Lifshitz–Gilbert equations. Exploiting the inverse Faraday effect, the light pulses act on the magnetic system as ultrafast magnetic field pulses. The solution of the linearized equations is also studied since it provides a good approximation for the magnetization in the regime of small field intensities and short times (of the order of ten picoseconds). Finally, the effect of weak damping is investigated since it is the most interesting for experiments involving the inverse Faraday effect and coherent interferential patterns are not completely destroyed.

First the excitation by double pulses is analysed. In the absence of damping, there is doubling or vanishing of the magnetization if the second pulse is in phase or out of phase with the magnetization, respectively. Relaxation weakens coherent effects and causes a reduction of the amplitude. The vanishing of the signal in the out-of-phase case is no longer achieved after the second pulse. However, if the intensity of the second pulse is decreased by an amount depending on the damping constant, the magnetization can vanish. Therefore, even in the presence of relaxation, a certain degree of control can be obtained.

For fields with intensity up to some teslas, nonlinear effects provide no contribution in the case of double pulses. When multiple pulses excite the system, nonlinear effects become important for smaller fields and hinder the possibility of coherent control. Different physical regimes can be analysed. In the linear regime without damping, in-phase pulses induce an increase of the magnetization by 100% after any excitation (pure coherent control). The effect of damping in the linear regime at first causes a reduction of the amplitude, but, after many pulses, the response enters a stationary regime. The magnetization shows a periodicity induced by the separation time between consecutive pulses and its amplitude depends on the damping time. Nonlinearity affects the magnetic response of the system after many pulses for field amplitudes of fractions of a tesla and after a few pulses for intensities of the order of 1 T. The magnetization is characterized by complex beating patterns whose amplitude and periodicity depend on the intensity of the exciting pulses. Finally, the combined role of nonlinearity and damping is analysed. After many pulses, a stationary solution characterizes the behaviour of the magnetization as in the linear regime. However, due to nonlinearity, saturation effects on the amplitude are present for fields with intensity of the order of 1 T. On the scale of hundred picoseconds in the presence of nonlinear effects, the coherent control of magnetization turns out not to be trivial even for magnetic field pulses whose intensity is not large.

The outline of this paper is as follows. In the next section the dynamical equations are presented together with the analytic solution of the linearized system and the calculation procedure. Sections 3 and 4 contain the discussion about the excitation by double and multiple pulses, respectively. Section 5 provides a summary.

2. Dynamical equations and linearized solution

The inverse Faraday effect has been observed in insulating magnets, such as canted antiferromagnetic dysprosium orthoferrites [5] and ferrimagnetic garnet films [9]. It has been possible to show experimentally coherent optical control of magnetization via the inverse Faraday effect with double pump pulses in garnet films [10] and rare-earth orthoferrites [12]. In this paper, rare-earth orthoferrites are studied as a model system.

Rare-earth orthoferrites are iron oxides with a perovskite-type structure. The spins of iron ions are antiferromagnetically aligned through a strong exchange interaction which corresponds to an exchange field E of approximately 6.4×10^6 Oe [13]. The spin canted magnetism with a weak saturation moment is due to an antisymmetric exchange interaction whose magnitude is expressed by the exchange field D of the order of 1.4×10^5 Oe [13]. The most stable phase is called Γ_4 and has a net magnetic moment. A free energy was proposed in a previous work [14] in order to analyse resonances and susceptibility of the Γ_4 phase. This theory was later used by the authors of this paper in order to study the magnetization dynamics induced via the inverse Faraday effect with a single pump pulse [8]. The normalized free energy $V = F/M_0$, with M_0 the modulus of the sublattice magnetization,

$$V = V_{\text{exc}} + V_{\text{ani}}, \tag{1}$$

consists of a part V_{exc} due to exchange interactions and a part V_{ani} due to the anisotropy [14]. The exchange energy is given by the sum of a scalar and a pseudo-vector part

$$V_{\text{exc}} = E\vec{R}_1 \cdot \vec{R}_2 + D(X_1Z_2 - X_2Z_1), \tag{2}$$

where E and D are the symmetric and antisymmetric exchange fields, respectively, $\vec{R}_1 = \vec{M}_1/M_0 \equiv (X_1, Y_1, Z_1)$, and $\vec{R}_2 = \vec{M}_2/M_0 \equiv (X_2, Y_2, Z_2)$. The anisotropic energy is

$$V_{\text{ani}} = -A_{xx}(X_1^2 + X_2^2) - A_{zz}(Z_1^2 + Z_2^2). \tag{3}$$

The anisotropy constants A_{xx} and A_{zz} are of the order of hundreds of Oersted and depend on temperature. In the Γ_4 phase of dysprosium orthoferrites at low temperature, A_{xx} is estimated to be about −640 Oe and A_{zz} close to a value of −1540 Oe [8].

The equilibrium position of the magnetization in the Γ_4 phase corresponds to a minimum of the free energy (1). It is given by $X_1^{\text{eq}} = -X_2^{\text{eq}} = \cos(\beta_0)$ and $Z_1^{\text{eq}} = Z_2^{\text{eq}} = \sin(\beta_0)$, where the small canting angle β_0 is determined by

$$\tan(2\beta_0) = \frac{D}{E + A_{xx} - A_{zz}} \simeq \frac{D}{E} = 0.022. \tag{4}$$

Therefore, the sublattice magnetization vectors point in opposite directions and are slightly noncollinear [14]. The saturation magnetization along the z-axis is

$$M_S = |\vec{M}_1 + \vec{M}_2| = 2M_0 \sin(\beta_0) \sim 0.022M_0, \tag{5}$$

which is two orders of magnitude smaller than M_0.

The free energy V in (1) enters the nonlinear Landau–Lifshitz–Gilbert dynamical equations

$$\frac{d\vec{R}_1}{dt} = -\gamma\vec{R}_1 \wedge \left(\vec{H}(t) - \vec{\nabla}_1 V\right) + \alpha\vec{R}_1 \wedge \frac{d\vec{R}_1}{dt} \quad (6)$$

$$\frac{d\vec{R}_2}{dt} = -\gamma\vec{R}_2 \wedge \left(\vec{H}(t) - \vec{\nabla}_2 V\right) + \alpha\vec{R}_2 \wedge \frac{d\vec{R}_2}{dt}, \quad (7)$$

where $\gamma = 17.6$ MHz Oe^{-1} is the gyroscopic ratio, and $\vec{\nabla}_1$ and $\vec{\nabla}_2$ are gradients with respect to $\vec{R}_1$ and $\vec{R}_2$, respectively.

The quantity $\vec{H}(t)$ in equations (6), (7) is the time-dependent magnetic field simulating the effect of laser pulses via the inverse Faraday effect. The ultrafast magnetic field is optically generated by a stimulated Raman-like coherent scattering mechanism via virtual states with strong spin–orbit coupling [6, 7]. Within this second order process, the intermediate excited states are coupled to states in the ground-state manifold via dipole matrix elements and the strength of the laser electric field. The effective magnetic field is proportional to the modulus square of the electric field, i.e. to the intensity of the laser pulse. In the numerical simulations, pulses are directed along the propagation direction of the light and have Gaussian shapes:

$$\vec{H}(t) = \hat{k}\sum_{n=0}^{N-1} \frac{F_n}{\sqrt{\pi}\tau_p} \exp\left[-(t - T_n)^2/\tau_p^2\right], \quad (8)$$

where $\hat{k}$ defines the direction of the light wavevector, N is the number of pulses, T_n is the centre of the pulse n, and τ_p indicates approximately the duration of each pulse. The pulses are assumed equally spaced in time, i.e. $T_n = nT$, where T is the separation time between successive pulses (with $T \gg \tau_p$). Due to the dependence of the fields on intensity of the laser light, there is no phase correlation between pulses.

Finally, in equations (6), (7) α is the Gilbert constant. This quantity takes into account the damping of the oscillations, which, on the picosecond scale, is mainly caused by magnon–magnon scattering [8]. The values of α range from about 0.4×10^{-4} at $T = 50$ K to 3×10^{-4} at $T = 200$ K [8]. Therefore, the oscillations of magnetization are not strongly damped.

2.1. Solution of the linearized system

In this subsection the focus is on the solution determined by linearizing equations (6), (7) and the excitation of this linear system due to magnetic field pulses shaped as delta functions. This is a good approximation in the linear regime since the temporal pulse length is much smaller than the periods of the resonance modes. In the linearized form of equations (6), (7) the damping is introduced by using the relaxation time approximation. Therefore, the relaxation towards the equilibrium position is described by the damping time τ or, equivalently, the scattering rate $\Gamma = 1/\tau$ related to the quantity α.

In order to take into account small deviations from the equilibrium, the standard approach is to consider two separate coordinate systems, (S_1, T_1, Y_1) and (S_2, T_2, Y_2), which describe the dynamics of $\vec{M}_1$ and $\vec{M}_2$, respectively [14]. The variables S_1 and S_2 are chosen in order to coincide with the equilibrium positions of $\vec{M}_1$ and $\vec{M}_2$, respectively, so that

$$S_1 = \sin(\beta_0)Z_1 + \cos(\beta_0)X_1, \quad (9)$$

$$T_1 = -\cos(\beta_0)Z_1 + \sin(\beta_0)X_1, \quad (10)$$

and

$$S_2 = \sin(\beta_0)Z_2 - \cos(\beta_0)X_2, \quad (11)$$

$$T_1 = \cos(\beta_0)Z_2 + \sin(\beta_0)X_2. \quad (12)$$

By linearizing the equations, the system is characterized by two modes, the quasi-antiferro mode ω_z and the quasi-ferro mode ω_{xy}, involving cooperative motions of spins of the two sublattices [14]. The first one, with frequency given by

$$\frac{\omega_z^2}{\gamma^2} = 4EA_{xx} + 4A_{xx}(A_{xx} - A_{zz}) + D^2 \simeq 4EA_{xx} + D^2, \tag{13}$$

corresponds to a dynamic with antiferromagnetic components along the x- and y-axis, and one ferromagnetic component along the z-axis. The second mode, with frequency determined by

$$\frac{\omega_{xy}^2}{\gamma^2} = 4E(A_{xx} - A_{zz}) + 4A_{xx}(A_{xx} - A_{zz}), \tag{14}$$

is characterized by magnetization vectors along the x- and y-directions. Both ω_z and ω_{xy} are of the order of several cm^{-1}.

When the field pulses are along the z-direction, only the quasi-antiferro mode is excited. We get the following equations:

$$\frac{\mathrm{d}D_T}{\mathrm{d}t} = \gamma\left(2A_{xx} + D^2/2E\right)D_Y, \tag{15}$$

$$\frac{\mathrm{d}D_Y}{\mathrm{d}t} = \gamma(-2E)D_T + 2\gamma\cos(\beta_0)H_z \mathrm{e}^{(t-t_0)/\tau}, \tag{16}$$

with $D_T = (T_1 - T_2)\mathrm{e}^{(t-t_0)/\tau}$, $D_Y = (Y_1 - Y_2)\mathrm{e}^{(t-t_0)/\tau}$, and t_0 initial time. One can derive a second order equation for D_T:

$$\frac{\mathrm{d}^2 D_T}{\mathrm{d}t^2} + \omega_z^2 D_T = 2\gamma^2\cos(\beta_0)\left(2A_{xx} + D^2/2E\right)H_z \mathrm{e}^{(t-t_0)/\tau}. \tag{17}$$

Starting from the equilibrium position for times smaller than $t_0 = 0^-$, the solution of the equation is

$$D_T = (-2\gamma)R\cos(\beta_0)\int_{t_0}^{t} \mathrm{d}t_1 \sin\left[\omega_z(t - t_1)\right] H_z(t_1)\mathrm{e}^{(t_1-t_0)/\tau}, \tag{18}$$

with R given by

$$R = \sqrt{\frac{2A_{xx} + D^2/2E}{2E}}. \tag{19}$$

From the knowledge of D_T we can derive D_Y, the variables T and Y, and then X and Z.

The linearized system can be solved for pulses with arbitrary shape. Simple solutions are obtained when the magnetic field pulses are shaped as delta functions:

$$\vec{H}(t) = \hat{k}\sum_{n=0}^{N-1} F_n \delta(t - nT). \tag{20}$$

The analysis deals with the case of the field directed along the z-axis, since this corresponds to the most important geometry used in the experimental set-up [5]. The field along this direction is able to excite only the quasi-antiferro mode [8], whose oscillating behaviour is characterized by the period

$$T_0 = \frac{2\pi}{\omega_z}. \tag{21}$$

The quantity T_0 is of the order of a few picoseconds.

The ferromagnetic component of this mode is described by $\Delta\tilde{M}_Z(t)$, the magnetization along the z-axis with respect to equilibrium $\Delta M_Z(t)$ in units of M_0, i.e. $\Delta\tilde{M}_Z(t) = \Delta M_Z(t)/M_0$, with the quantity $\Delta\tilde{M}_Z(t)$ given by

$$\Delta\tilde{M}_Z(t) = Z_1(t) + Z_2(t) - (Z_1^{\mathrm{eq}} + Z_2^{\mathrm{eq}}). \tag{22}$$

In the time interval $(J-1)T < t < JT$, with J an integer smaller than N, $\Delta\tilde{M}_Z$ is given by

$$\Delta\tilde{M}_Z(t) = 2\cos^2(\beta_0)RG_J(t), \tag{23}$$

where $G_J(t)$ is

$$G_J(t) = \sum_{n=0}^{J-1}(\gamma F_n)\mathrm{e}^{-\Gamma(t-nT)}\sin[\omega_z(t-nT)]. \tag{24}$$

For $t > (N-1)T$ the solution is

$$\Delta\tilde{M}_Z(t) = 2\cos^2(\beta_0)RG_N(t). \tag{25}$$

The most important antiferromagnetic component of the quasi-antiferro mode is that along the x-axis, which is described by $\Delta\tilde{A}_X(t)$, the component with respect to the equilibrium in units of M_0 [8]. We define $\Delta\tilde{A}_X(t) = \Delta A_X(t)/M_0$ or equivalently

$$\Delta\tilde{A}_X(t) = X_1(t) - X_2(t) - (X_1^{\mathrm{eq}} - X_2^{\mathrm{eq}}). \tag{26}$$

Using again the linearized form of equations (6), (7) and delta pulses, in the time interval $(J-1)T < t < JT$, $\Delta\tilde{A}_X(t)$ is

$$\Delta\tilde{A}_X(t) = 2\cos(\beta_0)L_J(t), \tag{27}$$

where $L_J(t)$ is

$$L_J(t) = \sum_{n=0}^{J-1}(\gamma F_n)\mathrm{e}^{-\Gamma(t-nT)}\cos[\omega_z(t-nT)]. \tag{28}$$

For $t > (N-1)T$ the solution is

$$\Delta\tilde{A}_X(t) = 2\cos(\beta_0)L_N(t). \tag{29}$$

2.2. Calculation procedure

The nonlinear dynamical equations (6) and (7) have been numerically integrated through a fifth-order Runge–Kutta algorithm. Two methods have been followed. The first one has dealt with the integration at fixed small time step of the order of fractions of femtosecond. The second procedure has considered an adaptive grid with a time step depending on a tolerance factor [15]. The tolerance factor valid for each time step has been varied from 10^{-5} to 10^{-6}. For both methods, the integration with multiple pulses up to times of the order of a hundred picoseconds is quite demanding in comparison with the case of double pulses, but it is very stable.

In the experiments the magnetic field pulses have amplitude of the order of 0.5 T and time length of hundreds of femtoseconds [5, 9, 10]. Therefore, in the numerical calculations, the Gaussian fields are of the form given in equation (8), with $F_n = \sqrt{\pi}\tau_{\mathrm{p}}\mathrm{Amp}(H_n)$ and $\tau_{\mathrm{p}} = 200$ fs. The magnetic fields are directed along the z direction and their amplitudes $\mathrm{Amp}(H_n)$ range from 2000 to 16 000 Oe. We also consider fields a bit larger than those in experiments in order to highlight the role of nonlinear effects in the case of multiple pulses. In the simulations only the low-temperature values of the anisotropy constants given in the previous section are included. Their small temperature-dependent change is neglected since it is able to affect the frequency but not the amplitude of the magnetization [8]. The constant α is varied from zero up to 10^{-4} in order to analyse the effect of the damping on the coherent phenomena induced by multiple pulses. The separation time between two successive pulses is between 3 and 4 T_0, since these time intervals are close to those used in experimental measurements [12].

Since the time width τ_p of the single pulse is small on the scale of the mode periods, in the linear regime, the numerical results for the magnetization are in good agreement with those by equations (23) and (25) derived with delta pulses. The dynamics of magnetization is strongly correlated with the behaviour of the antiferromagnetic vector even if they have different magnitudes [8]. However, the solution of the linear system is not very accurate for the antiferromagnetic vector. Hence, in all the following figures, the plotted results are obtained by numerical integration.

In a previous study the role of nonlinear effects was checked by the authors of this paper for the case of a single pulse [8]. In the absence of damping, weak nonlinear effects appeared only for pulse intensities close to 20 T. These were much larger than fields induced via the inverse Faraday effect in the experiments, so that we did not discuss nonlinear contributions. In this case weak nonlinearity appeared as a distortion of the simple sinusoidal behaviour of the linear regime. Only with further increase of the intensity did some saturation effects in the amplitude of the ferromagnetic response become not negligible. In order to characterize the presence of nonlinear contributions, the procedure was to study the decreasing quality of the fit made with simple sinusoidal functions and the contribution by higher order harmonics of the mode frequency by using the fast Fourier transform (FFT). The same procedure is followed in this paper.

In the next section the effects of two Gaussian pulses along the z direction are discussed. In the subsequent section the focus is on the excitation by multiple magnetic field pulses. In both cases the system is in the Γ_4 phase before the arrival of the pulses.

3. Double pulses

In this section the excitation of the magnetic system by two pulses is studied. The role of the damping is analysed in this simple physical situation. Nonlinear effects provide no contribution for fields with intensity up to some teslas. These effects will be investigated in the next section as a consequence of multiple pulses.

The oscillating behaviour of the ferromagnetic vector along z due to double pulses is shown in figure 1(a). In the absence of damping, after the first pulse, the magnetization has a sine-like behaviour on the picosecond scale. The second pulse with the same amplitude as the first one acts after a time $T = T_d \approx 3T_0$, with T_0 given in equation (21). It is in phase with the previous signal, so that it gives rise to a perfect doubling of the magnetization. The symbol $\approx$ means that the centre of the second Gaussian pulse occurs at the indicated time. This behaviour is simply obtained from equation (25), which, without damping and for two equal pulses, yields for $T_d = mT_0$, with m integer, $G_2(t) = 2\gamma F_0 \sin(\omega_z t)$.

The role of damping in the double-pulse excitation is also shown in figure 1(a). The value $\alpha = 10^{-4}$ gives rise to weak damping during the first picoseconds. The fit of the first three periods of the magnetization with a damped sine function provides an estimate for the damping time: $\tau \simeq 88$ ps (equivalently $\Gamma \simeq 0.011$ ps^{-1}). After a time $T_d \approx 3T_0$, a second equal pulse excites the system. In the presence of small damping, the constructive effect is weakened and the amplitude after three periods shows departure from the ideal value of $\alpha = 0$. This behaviour can be easily described by using equation (25), which gives for $T_d = mT_0$, with m integer,

$$G_2(t) = 2\gamma F_0 \sin(\omega_z t) \left[\frac{e^{-\Gamma t}}{2} + \frac{e^{-\Gamma (t-T_d)}}{2} \right], \quad (30)$$

where the damping terms between brackets control the reduction of the amplitude. There is also an ‘asymmetry’ in the time intervals $0 < t < T_d$ and $T_d < t < 2T_d$ due to the role of damping. For a time $\bar{t}$ such that $0 < \bar{t} < T_d$, the amplitude decreases by the factor $\exp(-\Gamma \bar{t})$. Instead,

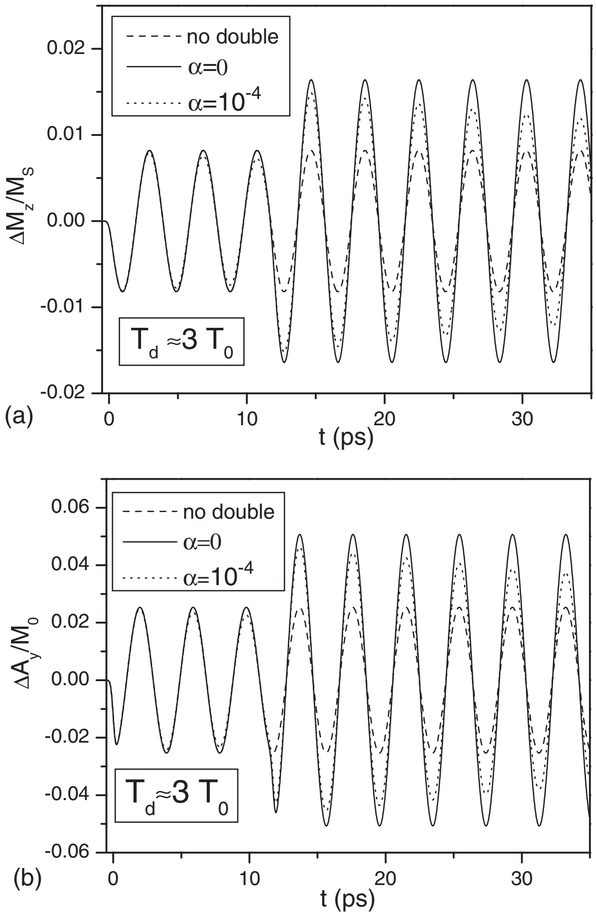

Figure 1. (a) The variation ΔM_Z of the magnetization along the z-axis with respect to the equilibrium value in units of M_S as a function of time for two values of the damping constant α. (b) The variation of the antiferromagnetic vector along the y-axis ΔA_Y with respect to M_0 as a function of time for two values of the damping constant α. In both cases the amplitude of both pulses is 2000 Oe and the dashed line shows the result without the effect of the second pulse.

for the time $\tilde{t} = \bar{t} + T_d$, the reduction is controlled by the factor $0.5\exp(-\Gamma\bar{t})[1+\exp(-\Gamma T_d)]$ smaller than $\exp(-\Gamma\bar{t})$. Therefore, there is an 'accumulation' of damping on the intervals of length T_d. This effect will be important when multiple pulses are considered in the presence of damping.

The dynamics of the antiferromagnetic component ΔA_Y shows features similar to those of the ferromagnetic component. As shown in figure 1(b), there is a strong relationship with the results of figure 1(a). Due to the coupling between the spins involved in the mode, without damping, there is a doubling of the signal after the second pulse. This occurs even if the response for the antiferromagnetic component is two orders of magnitude larger than the magnetization and is more sensitive to the shape of the pulse [8]. It is important to notice that the correlation between ferromagnetic and antiferromagnetic components will be maintained even for multiple pulses. Therefore, in the following, only the behaviour of the ferromagnetic component is shown.

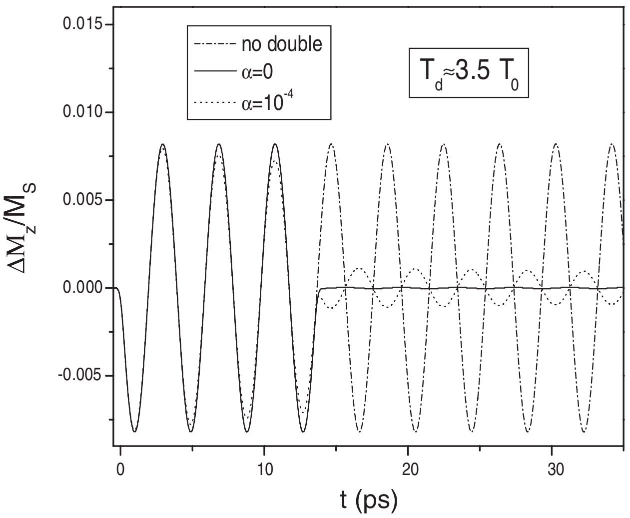

Figure 2. The variation ΔM_Z of the magnetization along the z-axis with respect to the equilibrium value in units of M_S as a function of time for two values of the damping constant α. The amplitude of both pulses is 2000 Oe and the dashed line shows the result without the effect of the second pulse.

The issue of destructive interference is addressed in figure 2. In this case the second pulse acts at the time $T_d \approx 3.5T_0$. In the absence of damping, the out-of-phase pulse causes the vanishing of the magnetization. Actually, for two equal exciting pulses and $T_d = mT_0 + T_0/2$, with m integer, equation (25) yields exactly $G_2(t) = 0$. As shown in figure 2, this condition is lost because of damping. Moreover, the presence of damping induces an inversion in the sign of the magnetization just after the second pulse. In order to explain the effect of damping, equation (25) can again be used, giving for $T_d = mT_0 + T_0/2$

$$G_2(t) = -\gamma F_0 e^{-\Gamma t} \sin(\omega_z t) \left(e^{\Gamma T_d} - 1\right). \tag{31}$$

For the case reported in figure 2, $T_0 \simeq 3.92$ ps and $T_d \approx 13.72$ ps. For $\alpha = 10^{-4}$, one gets $\Gamma T_d \simeq 0.15$, so that $\exp(\Gamma T_d) - 1 \simeq 0.16$. Therefore, in the regime of weak damping ($\Gamma T_d \ll 1$), the magnetization after the second pulse is not exactly zero, but is strongly reduced and inverts its sign. This result is obtained when the two pulses have equal amplitudes: $F_0 = F_1$. If the amplitude of the second pulse can be tuned, control of the magnetization can be obtained even in the presence of damping. One can fix $F_1 = \exp(-\Gamma T_d) F_0$: this condition provides the vanishing of the magnetization for $t > T_d$. The price to pay is that the amplitude of the second pulse has to depend on the excitation time T_d and the strength of the damping.

The results discussed in this section can be related not only to experiments performed in rare-earth orthoferrites but also in garnet films [10, 12]. Even though in garnets other magneto-optic effects can contribute to magnetic response, the role of the inverse Faraday effect to coherent phenomena seems to be pre-eminent. Considering that orthoferrites and garnets share iron–oxygen complexes as fundamental magneto-optical units, theoretical results obtained for orthoferrites also provide a qualitative picture for those in garnets. Finally, we notice that it is possible to have constructive or destructive interferential effects, even if the separation time and the helicity of the two pulses are fixed. In fact, an external static magnetic field can be used to directly tune the frequency of the mode excited by the first pulse. This is exploited in experiments [10]. This case could also be described within our approach since the

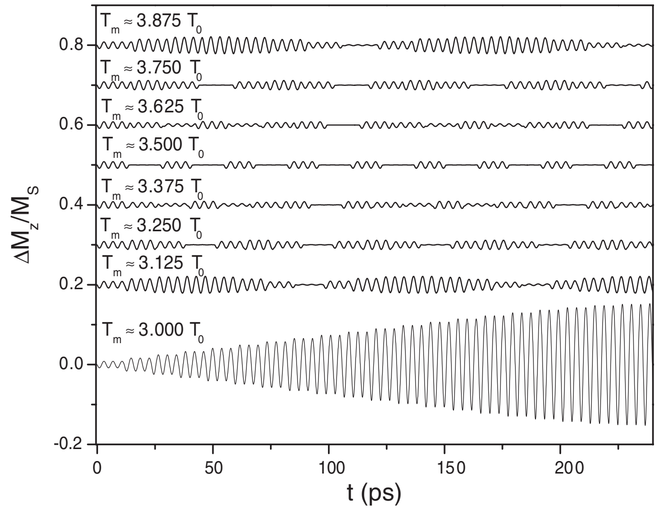

Figure 3. The variation ΔM_Z of the magnetization along the z-axis with respect to the equilibrium value in units of M_S as a function of time for several values of the separation time T_m in the absence of damping. The amplitude of each pulse is 2000 Oe.

dependence of the frequency of the quasi-antiferro mode on a static external magnetic field can be derived [14].

In the following only the issue of weak damping will be addressed, since this is the only regime related to experiments with inverse Faraday effect [5, 10]. The strong-damping regime is not interesting since the condition $\Gamma T_d \gg 1$ leads to a complete destruction of interference effects and the relaxation of the magnetization toward the equilibrium position is almost complete before the subsequent pulse arrives. Clearly, the aim is not to discuss phenomena such as spin echo where interference effects do not disappear if damping is caused by an inhomogeneous broadening [16].

4. Multiple pulses

In this section the analysis focuses on the effects of the excitation due to multiple pulses with equal amplitudes ($F_n = F_0$ for any n). In the first subsection the case of the absence of damping is studied, in the second subsection the role of damping is analysed.

4.1. Absence of damping

In the absence of damping, multiple pulses with different separation times $T = T_m$ give rise to several patterns. The results for T_m changing from $3T_0$ up to $4T_0$ are shown in figure 3 considering a field intensity of 2000 Oe. The oscillations are sizable only for in-phase pulses, $T_m \approx 3T_0$, and, after J pulses, the amplitude becomes J times larger for times up to 200 ps. On the other hand, for out-of-phase pulses, $3T_0 < T_m < 4T_0$, the amplitudes are small and show a periodicity that depends on the time T_m of the pulses. For example, in the case $T_m \approx 3.5T_0$ the magnetization pattern has an effective period of $7T_0$. Therefore, the net effect of equally spaced multiple excitations is to increase the selectivity of the system response [17]. One has the possibility to amplify the signal generated by the first pulse (magnetization oscillations with period T_0) and minimize other effects. On the timescale of 100 ps, the only relevant amplitude is that for $T_m \approx 3T_0$.

The behaviour shown in figure 3 can be explained within the linear response. The results are fully described via equation (25), which, without damping, yields for the time interval $(J-1)T_{\rm m} < t < JT_{\rm m}$

$$\frac{G_J(t)}{\gamma F_0} = \frac{\sin(\omega_z T_{\rm m} J/2)}{\sin(\omega_z T_{\rm m}/2)} \sin\left(\omega_z \left[t - \frac{(J-1)T_{\rm m}}{2}\right]\right). \tag{32}$$

Therefore the oscillations with frequency ω_z are modulated by an amplitude term depending on the time $T_{\rm m}$ and J. For $T_{\rm m} = iT_0$, with i integer, one obtains the simple result $G_J(t) = J\sin(\omega_z t)$. Therefore, if one uses N pulses, the amplitude of the magnetization increases by a factor N in comparison with that after the first pulse. In the linear regime, this coherent control is due to the constructive interference of all the pulses up to $(N-1)T_{\rm m}$. As soon as the condition $T_{\rm m} = iT_0$ is not fulfilled, different kinds of amplitude modulation can be obtained (see figure 3).

The discussion up to now has been limited to the linear regime. However, the dynamical equations (6) and (7) are not linear. Hence, one expects that nonlinear effects can take place after many in-phase pulses, when the amplitude of the magnetic response starts being comparable with the magnetization $M_{\rm S}$. In figure 3, for times of the order of 200 ps, the in-phase oscillations ($T_{\rm m} \approx 3T_0$) show a saturation at a value that is about $0.15M_{\rm S}$. Therefore, even if the single pulses are small, after many excitations the nonlinearity of the equations affects the magnetization. It is worth studying dynamics induced by in-phase pulses. We have found that the saturation of the amplitude is only a transient part of the effect due to nonlinearity. In figure 4(a) the results for $T_{\rm m} \approx 3T_0$ and several intensities of the pulses are presented. The effects of the nonlinear terms strongly affect the magnetization dynamics on the picosecond scale. Due to nonlinear effects, the in-phase oscillations show complex beating patterns. At fixed intensity, it has been possible to verify that, up to the nanosecond, the shape of these patterns is periodically repeated. However, their amplitude is strongly dependent on the intensity, which controls periodicity and length. Clearly nonlinear effects limit the coherent control of magnetization.

In figure 4(b) the focus is on the plot corresponding to the multiple pulses with the largest amplitude. The analysis of the oscillations reveals how the nonlinear effects give rise to these complex behaviours. In the figure the arrows indicate the times when the pulses act on the system. The horizontal bars denote the amplitude of the oscillations in the linear approximation. For the first four pulses the amplitudes of the magnetization follow the linear regime increasing at each step with a rate of 100%. However, the periods of the oscillations change after the excitation of the fields and the equally spaced pulses do not excite the system perfectly in phase. In order to analyse this effect, it is interesting to perform a fit of the oscillations in the time intervals $(J-1)T_{\rm m} < t < JT_{\rm m}$ with the simple sine function $A\sin[\pi(t-t_{\rm c})/w]$, where A is the amplitude, $t_{\rm c}$ is the time shift, and w is the half-period. After the first pulse the fit is excellent ($\chi^2 \simeq 3\times10^{-6}$) with $t_{\rm c} \simeq 0$ ps and $w \simeq 1.96$ ps. This corresponds to the result of the linear regime. After the third pulse the fit gets worse ($\chi^2 \simeq 8.2\times10^{-4}$) and provides $t_{\rm c} \simeq -0.25$ ps and $w \simeq 1.99$ ps. Therefore there is a marked time shift of the initial oscillation and an increase of the period of the oscillations. After the fifth pulse, the oscillations show only two maxima, which are smaller than the value predicted by the linear response (the horizontal bar is higher). The quality of the fit continues to decrease ($\chi^2 \simeq 3.8\times10^{-3}$), and the estimates are $t_{\rm c} \simeq -0.83$ ps and $w \simeq 2.03$ ps. Hence, after the fifth pulse, the time shift is close to $T_0/4$ and the period has increased. This is in agreement with the fact that there are only two maxima. Moreover, the value of the time shift is compatible with the periodicity of the pattern. Actually, after the next pulse, the amplitudes of the oscillations can change their increasing trend and start decreasing. After the seventh pulse, the amplitude is slightly smaller than that after the

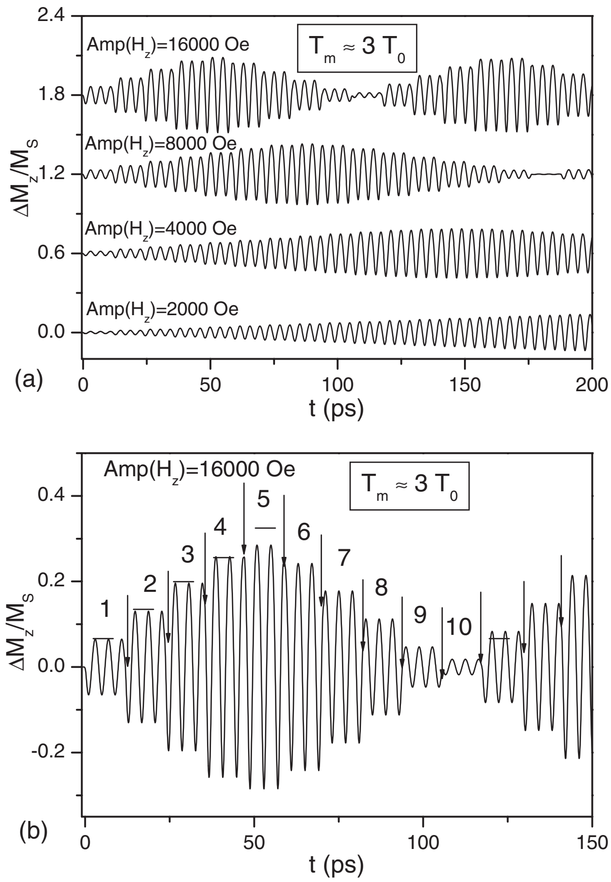

Figure 4. (a) The variation ΔM_Z of the magnetization along the z-axis with respect to the equilibrium value in units of M_S as a function of time for $T_m \approx 3.0T_0$ and several amplitudes of the exciting field pulses. Every new curve is shifted from the previous one along the vertical axis over 0.6. (b) The variation ΔM_Z of the magnetization along the z-axis with respect to the equilibrium value in units of M_S as a function of time for $T_m \approx 3.0T_0$ for field intensity equal to 16 000 Oe. Arrows indicate the times of pulse arrival.

third pulse, and the fit with the sine function has similar accuracy ($\chi^2 \simeq 5.2 \times 10^{-4}$). The time shift $t_c \simeq 0.52$ ps is positive and in modulus decreases in comparison with that after the fifth pulse. The period is also decreasing: $w \simeq 1.99$ ps. Therefore, there is a strong symmetry of the pulses after and before the fifth one. After the tenth pulse the fit is excellent ($\chi^2 \simeq 3.2 \times 10^{-6}$) and the period shows a value characteristic of the linear regime ($w \simeq 1.96$ ps). However, the time shift is large: in fact, $t_c \simeq 1.86$ ps, of the order of $T_0/2$. This means that the system is ready to start a new cycle with increasing amplitudes. Actually, this occurs after the 11th pulse with an amplitude not equal but very close to that after the first pulse. This pattern of cycles is repeated up to 1 ns with negligible modifications. The same behaviour is also found for multiple pulses with smaller amplitudes. However, as shown in figure 4(a), close to the maximum, the saturation lasts for many cycles, and more slowly the amplitudes start decreasing.

Stimulated by these findings, an analysis of the oscillations based on the FFT has been performed in any interval $(J-1)T_m < t < JT_m$ for amplitude equal to 16 000 Oe. Indeed, the fit with the sine function gets worse after some pulses, since the components of the oscillations at zero and double frequency $2\omega_z$ become not negligible. In the worst case, i.e. after the fifth pulse, the component at ω_z is about 0.19 M_S, that at zero frequency about 0.07 M_S and that at $2\omega_z$ is 0.06 M_S. Therefore, the role of higher harmonics of the fundamental ω_z and the component at zero frequency gain importance close to the maximum of the pattern. This explains the worst quality of the fit for this cycle. The same analysis shows similar results for smaller amplitudes of the exciting pulses.

4.2. Presence of damping

In this subsection the discussion focuses on the role of the damping in the linear and non-linear regimes when multiple pulses excite the system.

Unlike the case of two pulses, the damping can have profound effects on the magnetization dynamics even if it is very small. Actually, the damping time should not be compared only with the excitation time T_m of the pulses, but also with the duration time JT_m of J pulses. Even if $\tau = 1/\Gamma$ is larger than T_m, after many pulses the damping time becomes smaller than JT_m. As shown in figure 5(a), after the initial pulses the magnetization starts increasing as in the linear regime in absence of damping. The only difference is that, after pulse J, the amplitude is slightly smaller than J times the amplitude after the first pulse. However, after many pulses the magnetization tends toward a stationary solution, i.e. it is the same after any exciting pulse. This can be understood by using equation (23) valid in the linear regime. Actually, in the time interval $(J-1)T_m < t < JT_m$, one gets in the case of constructive interference, $T_m = iT_0$,

$$\frac{G_J(t)}{\gamma F_0} = e^{-\Gamma t}\frac{\left(e^{JT_m\Gamma}-1\right)}{\left(e^{T_m\Gamma}-1\right)}\sin(\omega_z t). \tag{33}$$

In the limit of small damping ($\Gamma T_m \ll 1$) and after the initial pulses ($JT_m \ll \tau$), $G_J(t)$ is approximated by

$$\frac{G_J(t)}{\gamma F_0} \simeq J\left(1-\Gamma\left[t-\frac{T_m(J-1)}{2}\right]\right)\sin(\omega_z t). \tag{34}$$

Therefore, the amplitude depends on the exciting pulse J with a small decay due to damping. However, as stressed in the case of double pumps, there is an ‘accumulation’ of damping over the excitation cycles. This effect gives rise to another behaviour on longer times. Indeed, in the same damping regime, after many pulses ($JT_m \gg \tau$),

$$\frac{G_J(t)}{\gamma F_0} \simeq \frac{1}{\Gamma T_m}e^{-\Gamma[t-T_m(J-1)]}\sin(\omega_z t). \tag{35}$$

The amplitude becomes independent of the exciting pulse J: in fact, it is only determined by the parameters T_m and Γ. For the case reported in figure 5, $\Gamma \simeq 0.011$ ps^{-1} for $\alpha = 10^{-4}$ and $T_m \approx 13.72$ ps, so that $1/\Gamma T_m \simeq 6.6$. This value is in close agreement with the numerical results of the magnetization on the scale of 100 ps shown in figure 5(a). Therefore, in the linear regime, by manipulating the value of the excitation time T_m and choosing different damping times, the amplitude of the magnetization can reach a fixed value. Even if incoherent, a control of the magnetization is still feasible.

Finally, the discussion concerns the combined role of damping and nonlinearity. The behaviour is more complex, but, after many pulses, the system is always characterized by a stationary solution. As shown in figure 5(b), the amplitude of the pulses also plays an important role. Actually, for small amplitudes of the pulses (2800 Oe), the effects of the nonlinearity are not so important since they affect the magnetization at long times when the stationary solution is already reached. For intermediate amplitudes of the excitation (5600 Oe), the effects due to nonlinearity and damping are strongly mixed. Finally, for large amplitudes of the field

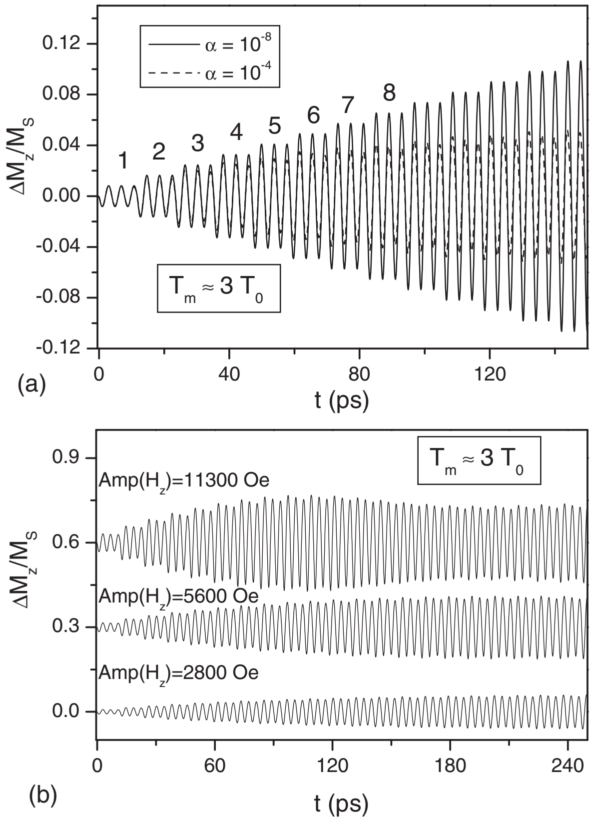

Figure 5. (a) The variation ΔM_Z of the magnetization along the z-axis with respect to the equilibrium value in units of M_S as a function of time for $T_m \approx 3.0T_0$ and the amplitude 2000 Oe of the exciting field pulses. (b) The variation ΔM_Z of the magnetization along the z-axis with respect to the equilibrium value in units of M_S as a function of time for $T_m \approx 3.0T_0$ and several amplitudes of the exciting field pulses. Every new curve is shifted from the previous one along the vertical axis over 0.3.

(11 300 Oe), the system shows the initial part of the pattern characteristic of the nonlinear regime. However, the cycles with decreasing amplitudes are not completed since the damping effect starts affecting the dynamics. There is also a saturation effect of the amplitude in the stationary regime for large fields. Indeed, over long times, the amplitude of the magnetization ranges from $0.057M_S$ just after fields of 2800 Oe, to $0.11M_S$ just after fields of 5600 Oe, then to only $0.13M_S$ for field amplitudes of 11 300 Oe. Therefore, passing from intermediate to strong field pulses, no doubling of the amplitude is obtained in the stationary regime. The control of magnetization is not trivial in the regime where damping and nonlinearity act together.

5. Summary and conclusion

Stimulated by experimental results showing ultrafast non-thermal control of magnetization by ultrafast laser pulses, a theoretical study about coherent manipulation of magnetization has been presented in this paper. Coupled sublattice nonlinear Landau–Lifshitz–Gilbert equations have been solved within an approach that has been recently proposed for the analysis of inverse

Faraday effect due to a single pump pulse in rare-earth orthoferrites [8]. The simulations have considered the effect of double and multiple pulses. The non-linear dynamical equations have been integrated through an optimized Runge–Kutta algorithm and analytical solutions of the linearized system have been discussed in the case when the magnetic field pulses have the shape of delta functions. The regime of weak damping has been studied due to its relation to the experiments.

First, the effect of double pulses was studied in the absence of damping. The behaviour of the magnetization is determined by the interference of the signals by the two pulses. Relaxation weakens coherent effects, but it allows a certain degree of control of magnetization with out-of-phase pulses. When multiple pulses excite the system in the linear regime without damping, an increase of the magnetization by 100% is achieved after any excitation. The effect of weak damping is not restricted to a decrease of the amplitude of magnetization. After many pulses, there is an 'accumulation' of damping effects that gives rise to a stationary behaviour of magnetization. The periodicity of magnetization is related to the separation time between consecutive pulses. The possibility of coherent control of magnetization is not only hindered by damping, but also by nonlinearity. The magnetic response of the system shows complex behaviours with amplitudes and periodicities depending on the intensity of the exciting pulses. Moreover, in the stationary regime induced by relaxation, a saturation effect characterizes the amplitude of the magnetization because of nonlinear terms.

Coherent control discussed in this paper is due to effective magnetic fields generated by light pulses via the inverse Faraday effect. Coherence effects can be also exploited in nuclear magnetic resonance (NMR) with pulses in the range of radio frequencies or microwaves [16]. In NMR experiments one-photon magnetic dipole spin-flip transitions are involved in order to stimulate spin precession. On the other hand, in optical experiments, spin precession is triggered via two-photon processes, similar to stimulated Raman scattering. Spin-flip transitions become allowed in electric-dipole approximation, thus should be more effective. Birefringence effects could hinder complete coherent control of magnetization in rare-earth orthoferrites; however, in optical experiments, manipulations of the laser pulses can be used in order to drive the two-photon process.

As a result of this study, the experimental conditions and the timescales useful for coherent manipulation can be specified. In rare-earth orthoferrites temperatures up to 100 K should not destroy coherent effects on the timescale up to 100 ps. In the experiments the Faraday rotation used to estimate magnetization dynamics shows nonthermal effects together with small thermal features [5]. However, the difference between the Faraday rotations induced by right- and left-handed polarized pulses minimizes nonthermal contributions. This difference can be properly used to investigate coherent control even in the presence of multiple pulses.

Acknowledgments

It is a pleasure to thank A V Kimel, A Bringer, and S Woodford for critical reading of the manuscript. CAP acknowledges financial support by the European RTN network DYNAMICS.

References

[1] Beaurepaire E, Merle J-C, Daunois A and Bigot J-Y 1996 *Phys. Rev. Lett.* **76** 4250
[2] Hohlfeld J, Matthias E, Knorren R and Bennemann K H 1997 *Phys. Rev. Lett.* **78** 4861
[3] Scholl A, Baumgarten L, Jacquemin R and Eberhardt W 1997 *Phys. Rev. Lett.* **79** 5146
[4] Koopmans B, van Kampen M, Kohlhepp J T and de Jonge J T 2000 *Phys. Rev. Lett.* **85** 844
[5] Kimel A V, Kirilyuk A, Usachev P A, Pisarev R V, Balbashov A M and Rasing Th 2005 *Nature* **435** 655

[6] Van der Ziel J P, Pershan P S and Malmstrom L D 1965 *Phys. Rev. Lett.* **15** 190
[7] Pershan P S, van der Ziel J P and Malmstrom L D 1966 *Phys. Rev.* **143** 574
[8] Perroni C A and Liebsch A 2006 *Preprint* cond-mat/0602593
[9] Hansteen F, Kimel A, Kirilyuk A and Rasing Th 2005 *Phys. Rev. Lett.* **95** 47402
[10] Hansteen F, Kimel A, Kirilyuk A and Rasing Th 2006 *Phys. Rev.* B **73** 014421
[11] Gomez-Alban R, Ney O, Satitkovitchai K and Hübner W 2004 *Phys. Rev. Lett.* **92** 227402
[12] Kimel A V 2006 private communication and unpublished results
[13] Koshizuka N and Hayashi K 1988 *J. Phys. Soc. Jpn.* **57** 4418
[14] Herrmann G F 1963 *J. Phys. Chem. Solids* **24** 597
[15] Nagle R K and Saff E B 1989 *Fundamentals of Differential Equations* 2nd edn (Redwood City, CA: Benjamin/Cummings)
[16] Slichter C P 1996 *Principles of Magnetic Resonance* 3rd edn (Berlin: Springer)
[17] Diels J-C and Rudolph W 1996 *Ultrashort Laser Pulse Phenomena* (New York: Academic)